

A THINNING ALGORITHM FOR EQUINE TENDON STRUCTURE IDENTIFICATION FROM 2D ULTRASOUND IMAGES

Ali Meghoufel¹, Guy Cloutier², Nathalie Crevier-Denoix³, and Jacques A. De Guise¹

¹École de Technologie Supérieure et Laboratoire de Recherche en Imagerie et Orthopédie, Centre de Recherche du CHUM, Montréal, Québec, Canada

²Laboratoire de Biorhéologie et d'Ultrasonographie Médicale, Centre de Recherche du CHUM, Montréal, Québec, Canada

³Biomécanique et Pathologie Locomotrice du Cheval, École Nationale Vétérinaire d'Alfort, France

ABSTRACT

In this paper, we propose a new shock filter algorithm for the thinning of hyperechoic structures observed on ultrasound (US) images of the equine superficial digital flexor tendon (SDFT). Implementation of the new algorithm is presented and applied on *in vivo* US data sets of a healthy and of an injured SDFT scanned with 7.5 MHz linear array transducer (SSD-2000-7.5, Aloka). Quantitative and qualitative results on the enhanced images show a coherent distribution of SDFT fiber bundles. In the case of normal SDFTs, the calculated number and area were respectively 48 ± 13 and $1.39 \pm 0.48 \text{ mm}^2$. In the case of injured SDFTs, the calculated number and area were respectively 40 ± 9 and $1.80 \pm 0.68 \text{ mm}^2$. The 3D reconstruction of the SDFT allowed a better assessment of the fiber bundles alignment along the SDFT loading axis, as well as the injured areas. In conclusion, segmentation results demonstrated the potential of the new thinning algorithm on the SDFT structure characterization.

Index Terms—Equine tendons, shock filter, thinning algorithm, ultrasound imaging.

1. INTRODUCTION

Ultrasound (US) is a widely used diagnostic technique to evaluate structures of the equine superficial digital flexor tendon (SDFT) after an injury and during the healing process [1]. However, the presence of speckle noise and artefacts affect interpretation of images as well as the accuracy of computer-assisted diagnostic techniques. The incomprehension of their contents makes feature extraction, analysis, recognition, and quantitative measurement difficult.

On transverse two dimensional (2D) US images corresponding to the cross-sectional area (CSA) of the SDFT (Figure 1), healthy SDFTs appear parallel and as linear hyperechoic structures [1, 2]. These echoes are caused by the coherent specular reflections at the interfascicular, which surround fiber bundles and are perpendicular to the US beam. In injured SDFTs, areas where fibres are disrupted appear as hypoechoic structures, due to the disorganization of the interfascicular and the loss in collagen density.

A number of methods have been addressed for speckle reduction and structure extraction from 2D US images including median filtering [3], adaptive speckle reduction filter [4], morphological operations [5], and Wavelet shrinkage [6]. The most

known methods for structure extraction from 2D US images are based on partial differential equations (PDE's) as nonlinear anisotropic diffusion [7]. The recent introduction of the PDE shock filter model [8, 9] may be a new method to segment US image contents accurately and efficiently. The shock filter is based on a deconvolution idea to create a sharp shock between two grey-scale zones on the image and produce piecewise constant segmentation. In this paper, a new shock filter algorithm is presented, which allows thinning of hyperechoic structures contained on 2D US images of the SDFT. The extraction of those structures and their quantification constitute information of great value for veterinarians because it enables appreciation of the structural integrity of the SDFT.

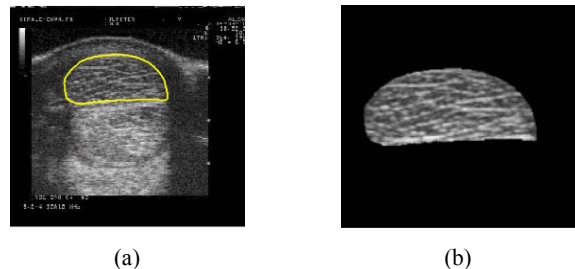


Figure 1: (a) 2D US image of a palmar tendon horse's hand, the SDFT region is identified, outlined, and zoomed in (b).

2. METHODS AND PROCEDURES

2.1. One dimensional deconvolution shock algorithm

The shock filter model proposed by Alvarez et Mazorra [8] in the one dimensional (1D) case is:

$$\begin{cases} u_t + F\left(\left(G_\sigma * u^0\right)_{xx}, \left(G_\sigma * u^0\right)_x\right) \cdot u_x = 0 \text{ in } \mathfrak{R} \times \mathfrak{R}^+ \\ u(x, t = 0) = u^0(x) \end{cases} \quad (1)$$

where G_σ is a Gaussian of standard deviation σ , u^0 and u are the original and the processed signals, $*$ is the convolution operator, and $F(\cdot, \cdot)$ is a function which should satisfy:

$$F(x, y) \cdot x, y \geq 0, \forall x, y \in \mathfrak{R}^2 \quad (2)$$

We set the following classical notations: $u_i^n = u(x_i = i\Delta x, t_n = n\Delta t)$, where Δx and Δt are respectively the spatial and time mesh sizes; u_i^n is the numerical approximation of u at the couple spatial and time points (x_i, t_n) , and $F_i = F\left(\frac{u_{i+1}^{0,\sigma} - 2 \cdot u_i^{0,\sigma} + u_{i-1}^{0,\sigma}}{\Delta x^2}, \frac{u_i^{0,\sigma} - u_{i-1}^{0,\sigma}}{\Delta x}\right)$, where $u^{0,\sigma} = G_\sigma * u^0$ is the smoothed original signal. The derivative scheme is an explicit upwind scheme [10]:

$$\begin{cases} \frac{u_i^{n+1} - u_i^n}{\Delta t} + F_i \frac{u_i^n - u_{i-1}^n}{\Delta x} = 0 \text{ if } F_i > 0 \\ \frac{u_i^{n+1} - u_i^n}{\Delta t} + F_i \frac{u_i^n - u_{i-1}^n}{\Delta x} = 0 \text{ if } F_i \leq 0 \end{cases} \quad (3)$$

Schematically, values u_i^{n+1} were obtained from values of u_k^n , where $k=i-1, i, i+1$ and from the initial smoothed original signal $u^{0,\sigma}$ expressed in the function F_i (Figure 2).

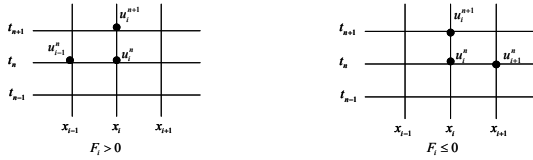


Figure 2: The explicit upwind scheme of the shock filter algorithm.

We resume the above numerical scheme of the hyperbolic equation (1) by the following simple explicit algorithm:

$$\begin{aligned} u_i^{n+1} &= u_i^n - \frac{\Delta t}{\Delta x} (\max(0, F_i) \cdot \Delta^+ u_i^n + \min(0, F_i) \cdot \Delta^- u_i^n) \\ \Delta^\pm u_i^n &= \pm (u_{i\pm 1}^n - u_i^n) \end{aligned} \quad (4)$$

The natures of results depend on the characteristics of the function F . For the classical case of the deconvolution shock algorithm, in which we create a discontinuity at inflexion points (i.e., zero-crossing of $u_{xx}^{0,\sigma}$), a simple choice for F that satisfies equation (2) is $F = F^1$:

$$F_i^1 = (\text{sign}(u_{xx}^{0,\sigma}) \cdot \text{sign}(u_x^{0,\sigma}))_i \quad (5)$$

where $\text{sign}(\cdot)$ is the sign function.

Figure 3 is an example showing the evolution of the deconvolution shock algorithm (the signal curve) for blur removal.

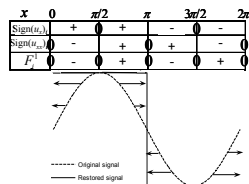


Figure 3: Restoration of a curved signal by the deconvolution shock algorithm after 30 iterations; $u^{0,0} = \sin(x)$.

The deconvolution shock algorithm offers better results than the traditional PDE technique as nonlinear anisotropic diffusion [7], for instance, we noticed the creation of a sharp shock at the inflexion points of the smoothed original signal, which is piecewise constant signal.

2.2. Hypothesis

Before evaluating the effectiveness of the proposed thinning shock algorithm, we pose assumptions in relation to our study. Indeed, the main objective of the study is to thin hyperechoic structures on 2D US images of the SDFT. The first assumption was to consider that the US image profiles are multimodal signals, i.e. they present hyperechoic structures. We also considered that points on which thinning should occur around them were those corresponding to the local maxima of the signals.

2.3. One dimensional thinning shock algorithm

A simple technique to characterize points corresponding to local maxima of the signal is to calculate the first derivative of the smoothed original signal $u^{0,\sigma}$. Locations of the zero crossing of $u_x^{0,\sigma}$ correspond to the curve of local extrema. Then, the process of shock thinning governed by the new function F will leave these extrema invariant, and it will make other pixels evolve/move according to their local properties (sign of the first derivative of the smoothed original signal). A simple choice for F that verifies equation (2) is $F = F^2$:

$$F_i^2 = \text{sign}(u_x^{0,\sigma})_i \quad (6)$$

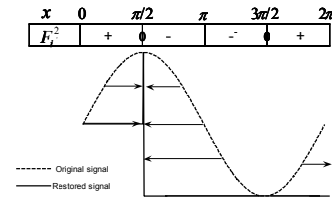


Figure 4: Skeleton of the 1D unimodal signal obtained by the thinning shock algorithm after 30 iterations; $u^{0,0} = \sin(x)$.

The following example (Figure 5) is the application of the deconvolution and thinning shock algorithms on a signal, which has inflexion points and many lobes (local maxima).

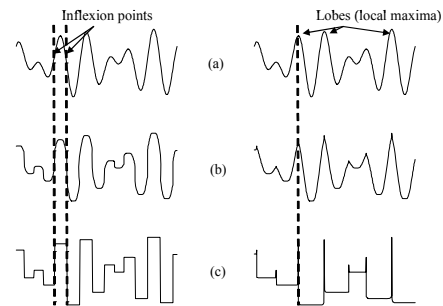


Figure 5: On the left panels, we show the solution by the deconvolution shock algorithm for the initial smoothed signal $u^{0,0} = \sin(5x) + \cos(7x)$. We notice discontinuities at the location of the zero crossing of $u_{xx}^{0,0}$. On the right panels, we show the solution by the thinning shock algorithm applied to the same signal $u^{0,0}$. It is shown that the thinning occurs at the location of the local maxima of $u^{0,0}$: (a) original signal; (b) signal sequence at iteration 8; and (c) signal sequence at iteration 30.

2.4. Two-dimensional thinning algorithm

The 2D shock filter model proposed by Alvarez and Mazorra [8] is composed of two parts : an anisotropic diffusion and a shock filter. In our study, we ignored the anisotropic diffusion term and the 2D model was written as:

$$\begin{cases} I_t + F\left(\left(G_\sigma * I^0\right)_{\eta\eta}, \left(G_\sigma * I^0\right)_\eta\right) I_\eta = 0 \text{ in } \mathfrak{R}^2 \times \mathfrak{R}^+ \\ I(x, y, t = 0) = I^0(x) \end{cases} \quad (7)$$

where I^0 and I are the original and processed images, η is the direction of the gradient of I , i.e. $\eta = \nabla I / \|\nabla I\|$, ∇ is the gradient operator, $\|\cdot\|$ is Euclidian norm, F satisfies equation (2), and G_σ is a 2D Gaussian of standard deviation σ .

Before introducing our 2D thinning algorithm, we set the following notation: $I^{0,\sigma} = G_\sigma * I^0$ is the smoothed original image. The term $I_\eta^{0,\sigma}$ is approximated as gradient, i.e. $\|\nabla I^{0,\sigma}\| \simeq I_\eta^{0,\sigma}$ as described in [8]. The choice of the function F is based on the same consideration as the 1D case.

The 2D upwind scheme is established for deconvolution and thinning because it guarantees the detection of local extrema according to the choice of the F function. The 2D thinning algorithm is the following explicit scheme:

$$I_{i,j}^{n+1} = I_{i,j}^n - \Delta t \cdot R(I_{i,j}^n) \quad (8)$$

where:

$$\begin{cases} R(I_{i,j}^n) = \max(0, F_{i,j}^2) K^+(I_{i,j}^n) + \min(0, F_{i,j}^2) K^-(I_{i,j}^n) \\ K^\pm(I_{i,j}^n) = \sqrt{(\Delta_x^\pm I_{i,j}^n)^2 + (\Delta_y^\pm I_{i,j}^n)^2} \\ F_{i,j}^2 = \text{sign}(\nabla I)_{i,j} \\ \Delta_x^\pm I_{i,j}^n = \pm(I_{i\pm 1,j}^n - I_{i,j}^n), \text{ and } \Delta_y^\pm I_{i,j}^n = \pm(I_{i,j\pm 1}^n - I_{i,j}^n) \end{cases} \quad (9)$$

The proposed algorithm is unconditionally stable and convergent [10].

3. RESULTS

The application of the 2D thinning shock algorithm on the clinical 2D US images of the SDFT gave results similar to the 1D case. Thinning was done according to the gradient direction; and it was performed around the hyperechoic structures (local maxima) where they were left invariant. The results (Figure 6) show that the process converged well towards a bright thin interface. The thinning iterative process was based on a stop criterion conditioned by the error between two consecutive image sequences with a maximum of 50 iterations.

Figure 7 contains a close-up of the images in Figure 6 (boxed segments) including their corresponding 3D surfaces. The surface of the original segment (Figure 7-a) had two hyperechoic structures degraded by the speckles noise. The two surfaces corresponding to the segments after 20 and 30 iterations show that the thinning process removes speckles and the bright structures became finer and clearer (Figures 7-b and 7-c).

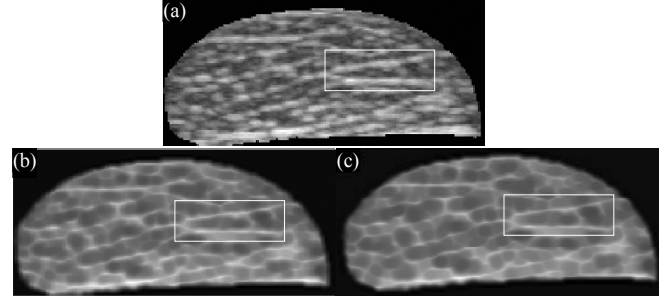


Figure 6: Thinning of the hyperechoic structure contained in the US image of the SDFT by the proposed 2D thinning shock algorithm: (a) original 2D US image of the SDFT after smoothing by a Gaussian operator with $\sigma = 2$; (b) image sequence at iteration 20; (c) image sequence at iteration 50.

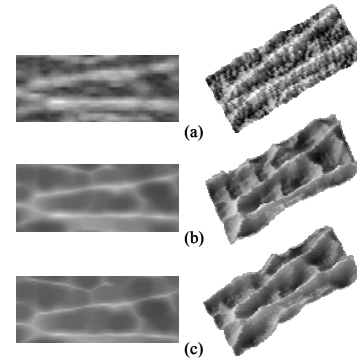


Figure 7: Segments (areas of interest) from images of figure 6 and their corresponding 3D surfaces: (a) original image segment; (b) segment at iteration 20; (c) segment at iteration 30.

To facilitate the extraction of quantitative information on fiber bundles, and also to improve the 2D and 3D visualization of the SDFT internal structure, a morphological closing operator was applied on the thinned hyperechoic structures by using the automatic ImageJ software function *Watershed* [11, 12] (Figure 8), as a final step of segmentation. A fiber bundle is defined as the smallest closed structure in the segmented image [1].

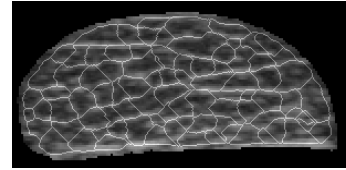


Figure 8: Superposition of the US image and closed hyperechoic structures by an automatic *watershed* operation [11].

Segmentation by the present algorithm was performed on *in vivo* US data sets of 8 healthy and 3 injured SDFTs scanned with a 7.5 MHz linear array transducer (SSD-2000-7.5, Aloka). Each data set had 120 ± 15 frames. Quantitative measurements are done on CSA of tendons to deduce the number of fiber bundles and the area

of each one. In the case of normal SDFTs, the calculated number and area were respectively 48 ± 13 and $1.39 \pm 0.48 \text{ mm}^2$. In the case of injured SDFTs, the calculated number and area were respectively 40 ± 9 and $1.80 \pm 0.68 \text{ mm}^2$. The determined area values corroborate those found by Gillis *et al.* [13] ($1.41 \pm 0.52 \text{ mm}^2$), who used an *in vitro* histomorphometric evaluation. Thirty successive segmented images were used to construct 3D views of the SDFT, from which the fiber bundles alignment along the SDFT loading axis (Figure 9), as well as the injured areas (Figure 10), can be assessed.

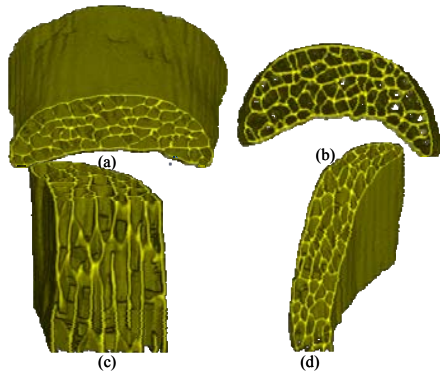


Figure 9: Different 3D views of a part of a healthy SDFT: (a) top view; (b) face view; (c) longitudinal cut of the tendon; and (d) oblique cut of the tendon.

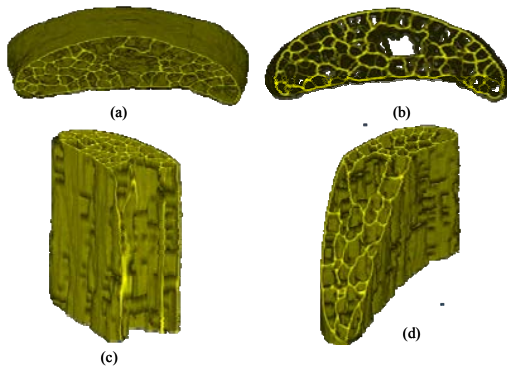


Figure 10: Different 3D views of a part of an injured SDFT: (a) top view; (b) face view; (c) longitudinal cut of the tendon; and (d) oblique cut of the tendon.

4. CONCLUSION

This study enabled us to be aware of the possibilities offered by the shock filter approaches in ultrasound image processing. Based on the numerical scheme of the Alvarez and Mazorra shock filter [8], we succeeded in modifying it to obtain encouraging results on the thinning of the hyperechoic structures contained in 2D US images of the SDFT.

The experimental results are promising and show that segmentation by the proposed thinning algorithm can provide a coherent 2D and 3D structures, from which the structural integrity of tendons can be appreciated. A large scale study should however be performed to fully validate the proposed method.

5. ACKNOWLEDGEMENTS

This study was supported by the *Natural Sciences and Engineering Research Council of Canada (NSERC)* and by the *Chaire de recherche du Canada en imagerie 3D et ingénierie biomédicale*.

6. REFERENCES

- [1] A. Meghoufel, N. Crevier-Denoix, G. Cloutier, and J. A. De Guise, "3D Tissue Characterization of the Equine Superficial Digital Flexor Tendons From In Vivo Ultrasound Images," 2006, pp. 2080-2083.
- [2] C. Martinoli, L. E. Derchi, C. Pastorino, M. Bertolotto, and E. Silvestri, "Analysis of Echotexture of Tendons with Us," *Radiology*, vol. 186, pp. 839-843, MAR 1993.
- [3] T. Loupas, W. N. Medicken, and P. L. Allan, "An adaptive weighted median filter for speckle suppression in medical ultrasonic images," *IEEE Trans. Circuits Syst*, vol. 36, pp. 129-135, 1989.
- [4] J. C. Bamber and C. Daft, "Adaptive filtering for reduction of speckle in ultrasonic pulse-echo images," *Ultrasonics*, vol. 24, pp. 41-4, Jan 1986.
- [5] P. Sladkevicius, L. Jokubkiene, and L. Valentin, "Contribution of morphological assessment of the vessel tree by three-dimensional ultrasound to a correct diagnosis of malignancy in ovarian masses," *Ultrasound Obstet Gynecol*, vol. 30, pp. 874-882, Oct 17 2007.
- [6] A. Aldroubi and M. Unser, "Wavelets in Medicine and Biology," *Boca Raton, FL: CRC*, 1996.
- [7] K. Z. Abd-Elmoniem, A.-B. M. Youssef, and Y. M. Kadah, "Real-time speckle reduction and coherence enhancement in ultrasound imaging via nonlinear anisotropic diffusion," *Biomedical Engineering, IEEE Transactions on*, vol. 49, pp. 997-1014, 2002.
- [8] I. Alvarez and L. Mazorra, "Signal and image restoration using shock filters and anisotropic diffusion," *SIAM J*, vol. 31, pp. 590-605, 1994.
- [9] S. J. Osher and L. I. Rudin, "Feature-oriented image enhancement using shock filters," *SIAM J. Numer. Anal.*, vol. 27, pp. 919-940, 1990.
- [10] J. A. Sethian and A. Vladimirsky, "Fast methods for the eikonal and related hamilton- jacobi equations on unstructured meshes," *Proc Natl Acad Sci U S A*, vol. 97, pp. 5699-703, May 23 2000.
- [11] L. Vincent and P. Soille, "Watersheds in digital spaces: an efficient algorithm based on immersion simulations," *Pattern Analysis and Machine Intelligence, IEEE Transactions on*, vol. 13, pp. 583-598, 1991.
- [12] W. Rasband, "ImageJ," 1.37 ed: National Institutes of Health, USA, 2007.
- [13] C. Gillis, R. R. Pool, D. M. Meagher, S. M. Stover, K. Reiser, and N. Willits, "Effect of maturation and aging on the histomorphometric and biochemical characteristics of equine superficial digital flexor tendon," *American Journal of Veterinary Research*, vol. 58, pp. 425-430, APR 1997.